

DIFFUSE DBD IN ATMOSPHERIC AIR AT DIFFERENT APPLIED PULSE WIDTHS

EKATERINA SHERSHUNOVA*, MAXIM MALASHIN, SERGEI MOSHKUNOV,
VLADISLAV KHOMECH

Institute for Electrophysics and Electric Power RAS, St. Petersburg, Russia, 191186, Dvortsovaya nab., 18

* corresponding author: eshershunova@gmail.com

ABSTRACT. This paper presents the realization and a diagnosis of the volume diffuse dielectric barrier discharge in a 1-mm air gap when high voltage rectangular pulses are applied to the electrodes. A detailed study has been made of the effect of the applied pulse width on the discharge dissipated energy. It has been found experimentally that the energy remained constant when the pulse was elongated from 600 ns to 1 ms.

KEYWORDS: dielectric barrier discharge; pulsed power supply; atmospheric pressure; pulse width; pulse energy.

1. INTRODUCTION

In recent years, much attention has been focused on realizing a diffuse atmospheric dielectric barrier discharge (DBD), and on investigating DBD, in association with its potential for use in plasma medicine, surface treatment, plasma chemistry, etc. Many researchers have shown that the diffuse mode of DBD with two discharge peaks per one voltage pulse can be ignited at low pressure, and even at atmospheric pressure, in gases such as neon, argon and helium by applying high voltage pulses with short durations to the electrodes [1, 2]. This increases the energy input into the discharge. There is no power consumption during the secondary discharge. At the same time, the energy stored at the barrier after the primary discharge is consumed.

As a rule, diffuse high-current DBD in atmospheric air is realized by applying voltage pulses of submicrosecond duration to the electrodes. There have been few studies on the influence of applying pulse width on DBD behavior in the microsecond range. In previous works, short bell-shaped pulses were used for initiating diffuse DBD in air [3, 4]. Only one primary discharge

pulse was clearly observed when applying these pulses. In our work, we present an experimental study, using a specially developed generator, of the influence of the applied pulse width on DBD development in atmospheric air.

2. EXPERIMENTAL SETUP

A special experimental setup was designed to generate a volume DBD in atmospheric air (Figure 1). Two special semiconductor switches S_1 and S_2 [5, 6] were used to supply DBD with rectangular voltage pulses with varying parameters: amplitude from 0 to 16 kV, pulse width from 600 ns to 1 ms, pulse repetition rates 1–3000 Hz. In addition, the rate of the rise of the applied voltage can easily be changed by varying the value of external resistor R_1 , thereby enabling the DBD mode to be controlled [7, 8].

DBD was initiated in a 1 mm atmospheric air gap (DG) under conditions of natural humidity of 40–60 % between two plane-parallel aluminum electrodes, one of which was covered by a 2 mm alumina ceramic plate at a pulse repetition rate of 30 Hz. The desired pulse width of the applied voltage was set by varying the

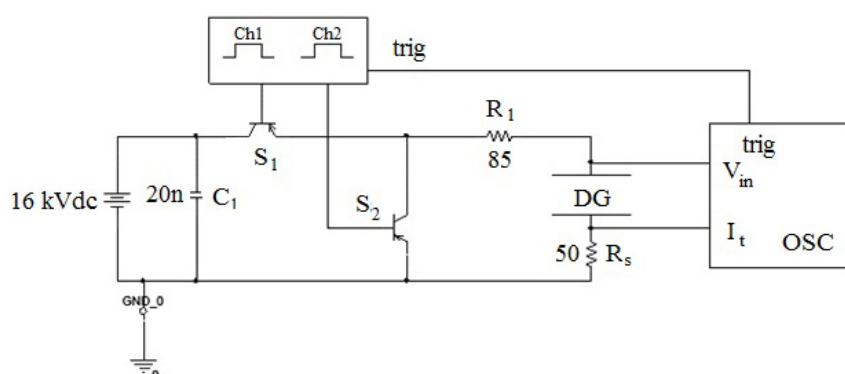


FIGURE 1. Experimental setup for realizing and diagnosing DBD.

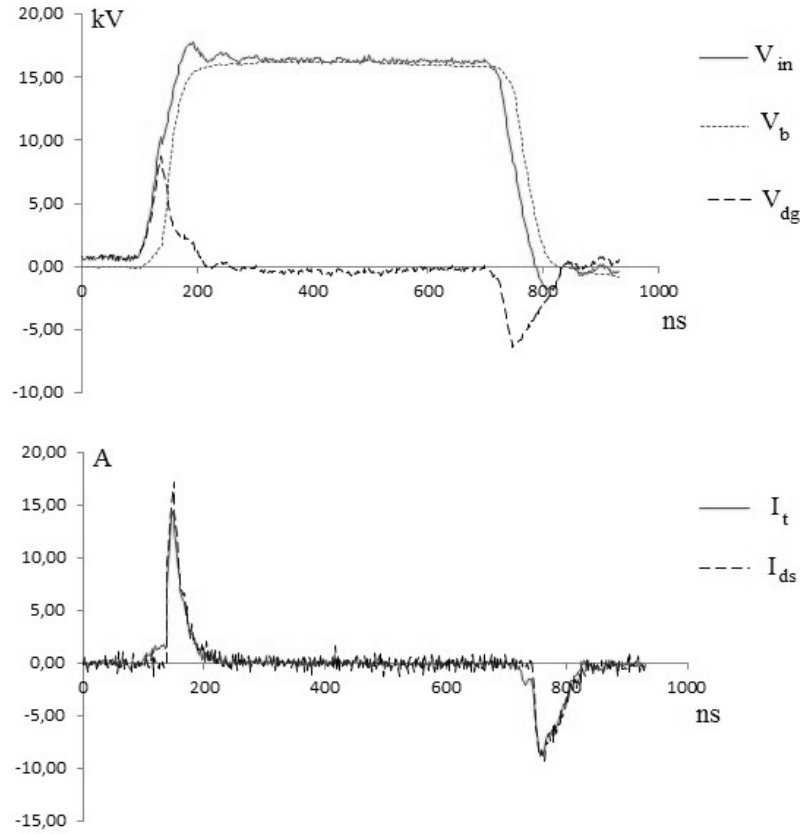


FIGURE 3. Experimental (V_{in} , I_t) and calculated (V_{dg} , I_{ds}) voltage and current traces of the volume diffuse DBD in a 1 mm air gap.

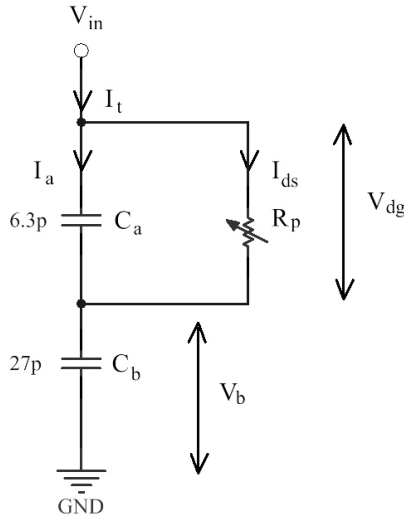


FIGURE 2. Equivalent circuit of DG.

time delay between triggering switches S_1 and S_2 . The voltage applied to the electrodes (V_{in}) was measured using a Tektronics P6015A high-voltage probe, and the total current in DG (I_t) was measured through the voltage drop at the $50\ \Omega$ series low-inductance resistor R_s . The voltage and current waveforms were displayed on a LeCroy WaveRunner oscilloscope (bandwidth 1 GHz, sampling rate 10 GS/s). The measured traces were the result of processing 1000 events.

3. CALCULATING THE ELECTRICAL AND ENERGY CHARACTERISTICS OF VOLUME DIFFUSE DBD IN ATMOSPHERIC AIR

The voltage drop for different elements of the discharge gap (DG), currents flowing through the circuit, discharge and supply power were evaluated according to the widely-used equivalent electrical circuit of the capacitive divider (Figure 2).

The voltage applied to the electrodes V_{in} and the total current in DG I_t , corresponding to the sum of the displacement current I_a (in the absence of a discharge) and the conduction current I_{ds} , are measured experimentally. From this data it is easy to calculate the voltage for the air gap V_{dg} and discharge current I_{ds} .

The voltage drop of the air gap is found by subtracting the voltage drop at the barrier V_b from the applied voltage V_{in} , using the formula $V_{dg} = V_{in} - V_b$, where $V_b = \frac{1}{C_b} \int I_t dt$ is the voltage at the barrier, I_t is the total current, and C_b is the capacitance of the barrier.

The discharge current is calculated from the difference between the total current and the current through the air capacitor C_a in the absence of the discharge: $I_{ds} = I_t - I_a$, where C_a is the capacitance of the air gap. The current through the air capacitor

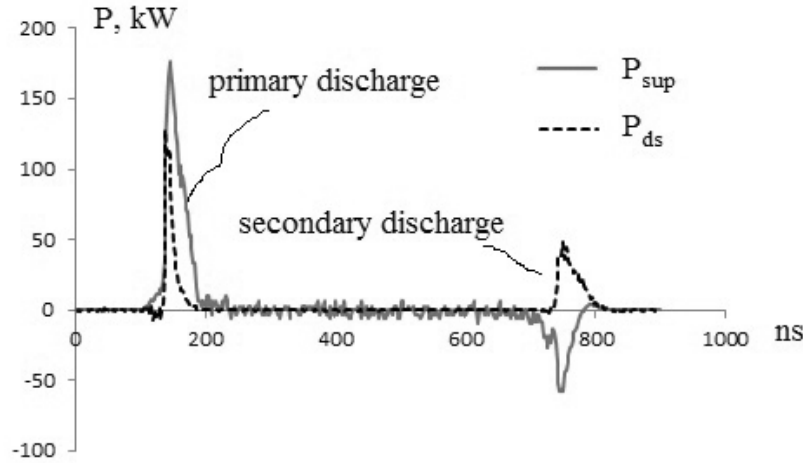


FIGURE 4. Externally supplied power P_{sup} and discharge dissipated power P_{ds} versus time, $t_p = 600$ ns.

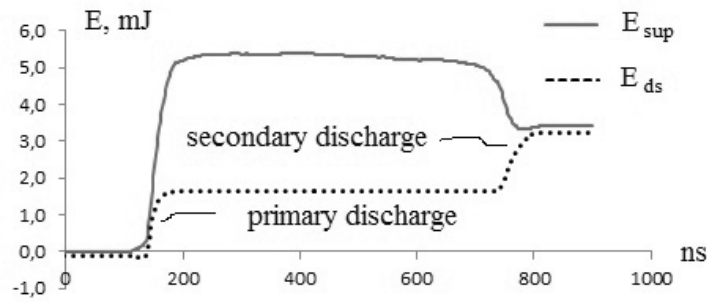


FIGURE 5. Temporal dependences of discharge energy E_{ds} and the energy from the external source E_{sup} ($V_{\text{in}} = 16$ kV, $t_p = 600$ ns, $h = 1$ mm, air, alumina ceramic barrier).

is obtained by multiplying the air capacitance and the time derivative of the voltage across the air gap, i.e., as $I_a = C_a \frac{dV_{\text{dg}}}{dt}$. Then, knowing the discharge current and the voltage at DG, the instantaneous power dissipated in the discharge P_{ds} can be calculated as $P_{\text{ds}} = I_{\text{ds}} V_{\text{dg}}$. Hence by integrating over time we find the discharge dissipated energy: $E_{\text{ds}} = \int P_{\text{ds}} dt$. The energy transferred from the external circuit can be estimated by the formula $E_{\text{sup}} = \int P_{\text{sup}} dt$, where $P_{\text{sup}} = I_t V_{\text{in}}$.

4. RESULTS

Figure 3 presents typical voltage and current waveforms of the volume diffuse DBD at $V_{\text{in}} = 16$ kV, $f = 30$ Hz, $R_1 = 85 \Omega$ and pulse width $t_p = 600$ ns.

As voltage V_{in} applies to the electrodes of DG, current I_t starts to flow through the circuit. Initially, this current charges the equivalent capacitance of DBD, which corresponds to a small hump at current trace I_t . When the voltage at the air gap V_{dg} exceeds the breakdown value, the primary discharge ignites. This looks like a sharp peak in the waveform.

The situation at the falling voltage edge is similar to the picture at the rising edge. First, the capacity of DBD is recharged, and then, when the breakdown voltage is exceeded, a discharge appears in DG, i.e. in the conduction current, corresponding the secondary

discharge pulse.

The time-dependences of the externally supplied power P_{sup} and the power dissipated in the discharge P_{ds} are shown in Figure 4.

Power comes from the external circuit (P_{sup}) to charge the equivalent capacitance of DBD and to the discharge process (P_{ds}). The secondary discharge pulse appears without direct consumption of power from the external source. This occurs due to the charge stored at the surface of the barrier after the primary discharge passes. The secondary discharge pulse leaves no charges on the barrier after it finishes. The calculated energy released in the primary discharge is about 1.8 mJ, and in the secondary discharge the calculated energy release is 1.5 mJ (Figure 5). Thus, the energy released per one pulse in the volume diffuse 1 mm DBD in air was ~ 3.3 mJ at the pulse width of the applied voltage of 600 ns.

We recorded the voltage and current traces for different pulse widths in order to compare the discharges. Figure 6 shows that with the elongation of the applied voltage pulse from 600 ns to 1 ms the peak current of the primary discharge remained constant at ~ 15 A, but the peak current of the secondary discharge increased slightly.

According to our experimental data, the charge transferred during the secondary discharge is constant

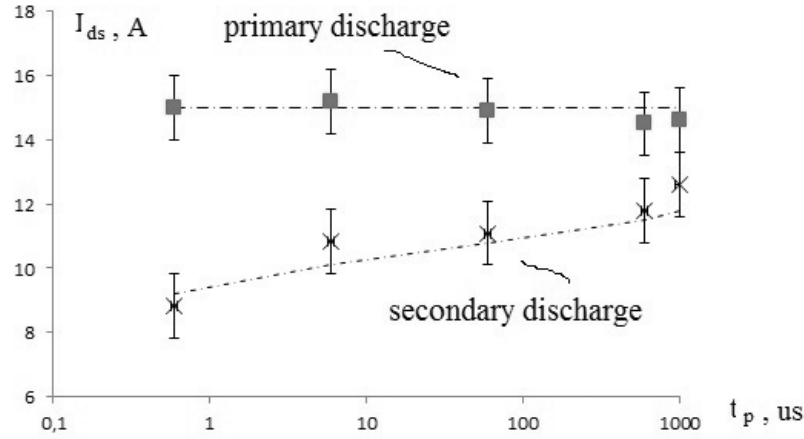
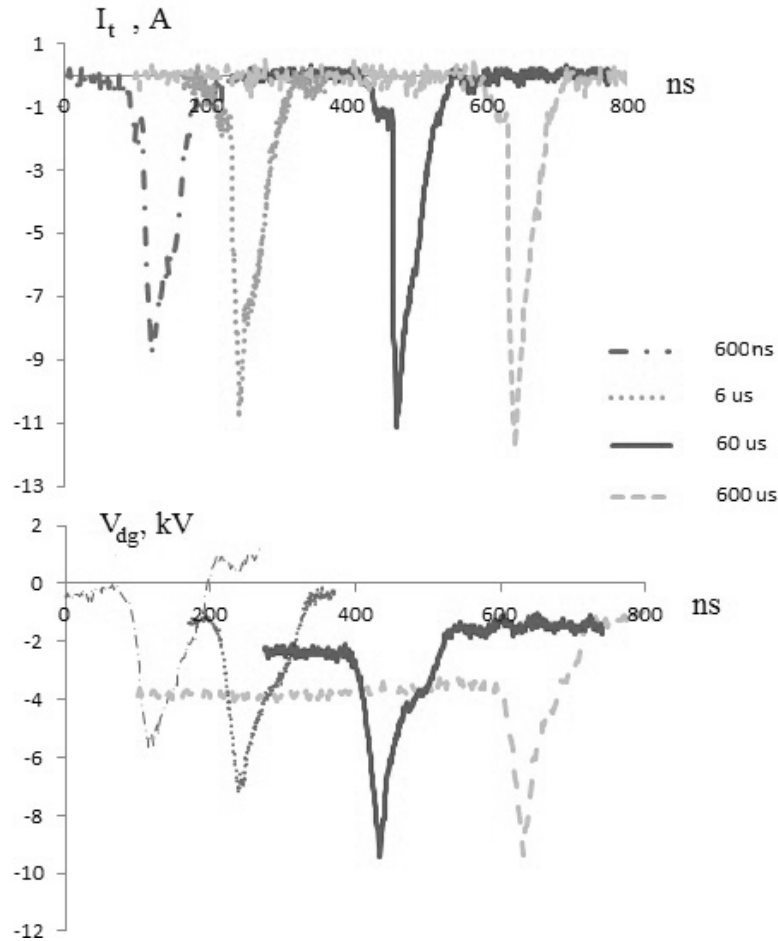


FIGURE 6. Dependences of primary and secondary discharge peaks versus pulse width.

FIGURE 7. Current I_t and voltage V_{dg} traces of the secondary discharge at different pulse widths.

with measured accuracy. We also consider the barrier capacitance to be constant. This allows the voltage at the barrier to be considered constant in the no-discharge period of the pulse. The voltage applied to DG V_{in} decreases due to the leakage current in the circuit, thus having an influence on the gap voltage. The growth of the secondary current pulse can therefore be explained by an increase in the gap voltage amplitude with pulse elongation (Figure 7).

The peak power of the primary discharge was about 150 ± 15 kW at any pulse width (Figure 8). The peak power of the secondary discharge changed twice as the pulse width increased from 600 ns to 1 ms. The total discharge energy in the pulse remained the same for any pulse width from the range. It was equal to 3.3 ± 0.1 mJ, where 1.8 mJ was dissipated in the primary discharge, and 1.5 mJ was dissipated in the secondary discharge.

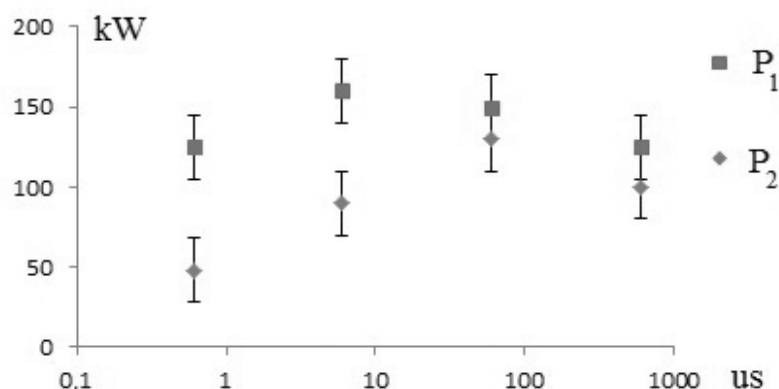


FIGURE 8. Peak discharge power (P_1 — primary discharge, P_2 — secondary discharge) versus pulse width.

5. SUMMARY

The volume diffuse DBD was realized in a 1 mm air gap when supplying the DG with rectangular unipolar voltage pulses 16 kV in amplitude, with a pulse repetition rate of 30 Hz at different pulse widths, from 600 ns to 1 ms. It was found experimentally that there was no correlation between the pulse width of the applied voltage and the energy dissipated in the discharge. The total dissipated discharge energy per pulse was about 3.3 mJ. It was also found that the slump in the applied voltage could cause an increase in the peak power of the secondary discharge.

ACKNOWLEDGEMENTS

The research work presented here was funded by the Russian Foundation for Basic Research, grant No. 1308-01043.

REFERENCES

- [1] Shuhai Liu, Manfred Neiger. Excitation of dielectric barrier discharges by unipolar submicrosecond square pulses. *Journal of Physics D: Applied Physics* **34**(11):1632, 2001. DOI:10.1088/0022-3727/34/11/312
- [2] XinPei Lu, Mounir Laroussi. Temporal and spatial emission behavior of homogeneous dielectric barrier discharge driven by unipolar sub-microsecond square pulses. *Journal of Physics D: Applied Physics* **39**(6):1127, 2006. DOI:10.1088/0022-3727/39/6/018
- [3] T. Shao, D. Zhang, Y. Yu, C. Zhang, J. Wang, P. Yang, Y. Zhou. A compact repetitive unipolar nanosecond-pulse generator for dielectric barrier discharge application. *IEEE Transactions on Plasma Science* **38**(7):1651-1655, 2010. DOI:10.1109/TPS.2010.2048724
- [4] H. Ayan, G. Fridman, A. F. Gutsol, V. N. Vasilets, A. Fridman, G. Friedman. Nanosecond-pulsed uniform dielectric-barrier discharge. *IEEE Transactions on Plasma Science* **36**(2):504-508, 2008. DOI:10.1109/TPS.2008.917947
- [5] V.Yu. Khomich, M.V. Malashin, S.I. Moshkunov, I.E. Rebrov, E.A. Shershunova. Solid-state system for Copper Vapor Laser Excitation. *EPE Journal* **23**(4):51–54, 2013.
- [6] M. V. Malashin, S. I. Moshkunov, I.E. Rebrov, V. Yu. Khomich, E. A. Shershunova. High-voltage Solid-State Switches for Microsecond Pulse Power. *Instruments and Experimental Techniques* **57**(2):140-143, 2014. DOI:10.1134/S0020441214010242
- [7] E. Shershunova, M. Malashin, S. Moshkunov, V. Khomich. Generation of Homogeneous Dielectric Barrier Discharge in Atmospheric Air without Preionization. *Abstract Book of the 19th Int. Vacuum Congress*. Paris, France. p. 1242, 2013. http://apps.key4events.com/key4register/images/client/164/files/Abstracts_IVC19.pdf [2014-12-01].
- [8] M. V. Malashin, S. I. Moshkunov, V. Yu. Khomich, E. A. Shershunova, V. A. Yamshchikov. On the possibility of generating volume dielectric barrier discharge in air at atmospheric pressure. *Technical Physics Letters* **39**(3):252-254, 2013. DOI:10.1134/S106378501303010